Journal of Polymers and the Environment (2021) 29:450–459
https://doi.org/10.1007/s10924-020-01886-6

ORIGINAL PAPER

Lignin-Based Polyethylene Films with Enhanced Thermal, Opacity and Biodegradability Properties for Agricultural Mulch Applications

Lucio R. Chiappero[1] · Suellen S. Bartolomei[2] · Diana A. Estenoz[3] · Esperidiana A. B. Moura[2] · Verónica V. Nicolau[1,4]

Accepted: 12 September 2020 / Published online: 21 September 2020

Abstract

Lignins are promising alternative raw materials for biocomposites due to their renewability, low cost and abundance. In this work, the use of (softwood and hardwood) Kraft lignins in the development of LLDPE/lignin films for agricultural mulch applications is studied. Processable blends were obtained from unmodified softwood lignin (SW) and from hardwood lignin modified by esterification (HWE). LLDPE was pelletized with (2.5%, 5% and 10%) lignin with particle size between 38 and 75 µm and flexible films were blown extruded. Processable extrusion blends showed temperature differences lower than 20 °C between the Tg of lignin and the melting temperature of LLPDE. Films from neat LLPDE and with 2.5% of HWE and up to 5% SW exhibited statistically comparable (≅ 349%) values of ductility. Ester groups present in lignin improve weight loss of lignin-based blends after soil buried test.

Keywords Kraft lignin · Mulch films · Extrusion · Esterification · Blends

Introduction

Plastic mulch film is a standard practice used in agriculture to control weeds, increase crop yield, and shorten time to harvest [1]. Most mulch films are currently produced from petroleum-based plastics, usually polyethylene (PE). Low density polyethylene (LDPE) and linear low density polyethylene (LLDPE) are mostly used in film production because of their high tear and impact strength [2]. Both are strong and flexible and have good transparency, moisture and gas barrier properties [3]. The long chain branching and the narrower molecular weight distribution of LDPE determine its greater transparency, gloss and better processability; whereas LLDPE has greater tensile and impact strength, better heat-seal properties, and lower cost. Films can be manufactured by extrusion, casting or blowing processes. The main advantage of blown films are their biaxial properties [4].

In order to reduce costs and/or improve some properties, particles such as calcium carbonate, silica and glass are added in thermoplastics. The size of the filler, the interfacial adhesion filler-matrix and the filler amount determine the final mechanical properties of the blends [5] Nanocomposite materials offer better combination of physical and mechanical properties than conventional materials.

Nowadays, there is a renewed interest in the use of organic fillers. Organic fillers, compared to inorganic fillers, have advantages such as low density, low abrasion, and its renewability. In this sense, lignin is a natural binder component of cellulose and hemicellulose present in the cell wall of all vascular plants with anti-UV and antioxidant properties and potential industrial use [6].

A great deal of research has been done on the use of lignin in polymeric matrix [7, 8]. Many reports have recently been published about lignin-based thermoplastic polymers [9]. The addition of lignin to thermoplastics has a double environmental and economic benefit.

✉ Verónica V. Nicolau
vnicolau@sanfrancisco.utn.edu.ar

1 GPol, Departamento de Ingeniería Química, Facultad Regional San Francisco, Universidad Tecnológica Nacional, Av. de la Universidad 501, San Francisco, Córdoba, Argentina

2 Center for Chemical and Environmental Technology (CQMA), Nuclear and Energy Research Institute (IPEN), Av. Prof. Lineu Prestes 2242, São Paulo, SP, Brazil

3 Instituto de Desarrollo Tecnológico Para la Industria Química, INTEC (UNL-CONICET), Güemes 3450, Santa Fe, SF, Argentina

4 Consejo Nacional de Investigaciones Científicas y Técnicas (CONICET), Godoy Cruz 2290, CABA, Argentina

Processing temperature, friction and shearing processes promote lignin overheating that result in its degradation and the emergence of black carbon. For this reason, proper processing conditions should be selected during the thermoplastic processing. Recently reports have shown that the combination of lignin with other thermally stable compounds, such as inorganic oxides (MgO, SiO_2, and ZnO) enables the development of novel composites for advanced applications [10–17]. Lignin in combination with inorganic fillers with good mechanical and thermal resistance, constitute a hybrid or dual filler that prevent aggregation and thermal degradation.

Lignin is abundant in nature and has a very complex random structure that varies depending on the species and the separation or pre-treatment processes [18]. In general, lignin is a copolymer derived from three basic phenylpropane monolignols: coniferyl alcohol, synapyl alcohol and p-coumaryl alcohol that lead to guaiacyl (G), syringyl (S) and p-hydroxyphenyl propane (p–H) moieties, respectively; linked by C–C and C–O–C linkages [19]. The G moieties are abundant in softwood lignin and can exceed 95% of the total moieties, meanwhile the ratio G/S decreases for hardwood lignin. The p–H moieties are almost negligible for wood lignin and similar proportions of G, S and p–H are present in herbaceous plants [20].

The pulp manufacturing process used by the paper industry determines the type of the available technical lignin, at least the most affordable at present. The three main chemical processes for the manufacture of cellulose pulp are sulfite, Kraft and soda [21]. Hardwood or softwood lignosulfonate, Kraft type lignin and soda type lignin differ in their chemical structure as well as in their physical and chemical properties. The characterization of lignin is complex due to the highly heterogeneous nature of the macromolecule.

The low compatibility between polar lignin and non-polar PE results in low miscibility and reduced mechanical properties of the materials [6]. In this sense, different methods have been developed in order to improve the compatibility. One strategy used in LLDPE/lignin blends, is the addition of coupling agents such as ethylene–vinyl acetate (EVA) [22] or maleic anhydride grafted PP and PE or a mixture of both [23]. The compatibility of blends promotes the improvement of mechanical properties of material [18]. A further strategy to enhance thermoplastic/lignin compatibility is the chemical modification of lignin by functionalizing the hydroxyl groups. Lignin contains phenolic hydroxyl groups and aliphatic hydroxyl groups at Cα and Cγ positions on the side chain. The chemical modification can be carried out by esterification, etherification, and by grafting and copolymerization reactions. Among all, esterification is an easy procedure to carry out considering the reaction conditions and reagents used [20]. Esterification increases the hydrophobicity of lignin, and therefore its solubility in organic solvents [24]. Esterification has already been used to improve the compatibility of lignin with HDPE [18], PLA [24, 25], PP [26, 27] and natural rubber latex (NRL) [28].

Lignin-based plastic mulch films must maintain the ability to be melt-processed, good mechanical properties such as tensile strength and elongation at break and good thermal properties. Also, biodegradability is a desired property to reduce environmental accumulation and pollution problem [29].

As far as the authors are aware, the information about the use of different types of lignin with LLDPE is scarce and even more about esterified lignin with LLDPE for mulch film applications. Comprehensive studies are necessary to generate knowledge associated to the structure–property relationship in LLDPE/lignin materials.

In this work, the preparation of blown films from LLDPE and a (softwood and hardwood) Kraft lignin of particle size 38–75 μm was studied. A chemical modification of the lignin by esterification reaction with acetic anhydride was also investigated in order to improve the compatibility and the processability of LLDPE/hardwood lignin blends via extrusion. Blends were characterized by spectroscopic, thermal and morphological analysis. Tensile strength, opacity and water absorption of films were measured. A soil biodegradation test was also performed for blends.

Materials and Methods

Materials

The polymer used in this study was LLDPE from Braskem (Brazil) in the form of pellets with a density of 0.931 g/cm^3 and a melting point of 122 °C. SW is a pine Kraft lignin, produced by MeadWestvaco Corporation, USA (Indulin-AT). HW is a eucalyptus Kraft lignin provided by Suzano Pulp and Paper, Brazil. Acetic anhydride (100%, Cicarelli) and N-methylimidazole (99%, Merck) were used for the esterification reaction. The reagents used in the characterization of lignin were dioxane (Cicarelli), NaOH (Cicarelli), KH_2PO_4 (Anedra), $Na_2B_4O_7{\cdot}10H_2O$ (Anedra), and methanol (Cicarelli).

Characterization of Lignin

The moisture and ash contents were measured by gravimetric techniques according to previously used methods [30] and the carbohydrate content was determined by High Performance Liquid Chromatography (HPLC) after hydrolysis of the lignin samples [21]. The lignin purity was calculated according to Eq. 1.

$$\text{Purity(dry basis)} = 100 - \%\text{ash (dry basis)} - \%\text{ carbohydrate (dry basis)} \quad (1)$$

An elemental CHNSO analyzer (SerieII, Perkin Elmer) was employed for the measurement of carbon (C), hydrogen (H), sulfur (S) and nitrogen (N) contents. Data were acquired using EA Data Manager 2400 software.

Size Exclusion Chromatography (SEC) was employed for molecular weights measurements. A Waters Liquid Chromatograph was employed to determine the average molecular weights of water insoluble lignin (SW), consisting of a 1525 binary pump model with a Waters 717 plus automatic injector, coupled to a set of Styragel HR 4E columns (7.8 × 300 mm) with a Waters 2414 differential refractive index detector. THF was used as the mobile phase with a flow rate of 1 mL/min. The system temperature was 25 °C. Polystyrene standards were used for the calibration.

For water soluble lignin (HW) a Waters Liquid Chromatograph was used, consisting of a Waters 1525 binary pump with a Waters 717 plus automatic injector, coupled to a set of 5 Ultrahydrogel columns of the following pore sizes: 120, 250, 500, 1000, 2000 Å and with a Waters 2414 refractive index detector. Buffer solution of pH 7.00 ($NaNO_3$ 0.1 M) was used as the mobile phase with a flow rate of 0.8 mL/min at room temperature. Polyethylene glycol was used as standard.

Phenolic hydroxyls were measured by UV spectroscopy [30]. Approximately 15 mg of unmodified lignin was weighed into a 10 mL flask and made up to the mark with dioxane. Then, 2 mL of the solution were transferred to three 50 mL flasks and made up to the mark with a buffer solution of pH 6, a buffer of pH 12, and NaOH 0.2 N. For the measurements a double beam UV–Vis Perkin Elmer Spectrophotometer Model Lambda 25 was used, using the lignin solution at pH 6 as reference solution. Then, the absorbances of the lignin solutions dissolved in NaOH 0.2 N and buffer solution of pH 12 were measured at 300 nm and at 360 nm.

Functional groups were analysed by Fourier Transformed Infrared spectroscopy (FTIR). The FTIR lignin spectra were acquired in a Shimadzu FTIR-8201 PC Fourier Transform Spectrophotometer in the 4000–400 cm^{-1} frequency region. KBr tablets containing 3%wt dry sample were prepared. Bands were assigned according to the literature [21, 31].

The solubility of the different types of lignin was obtained by dissolving 1 g of lignin in distilled water, THF and NaOH 0.1 N, respectively.

Glass transition temperature of lignin was determined by Differential Scanning Calorimetry (DSC) on a Mettler Toledo DSC 822 calorimeter. The sample was run from 0 to 200 °C and cooled down to 25 °C to remove any heat history and moisture. Then, the sample of lignin was heated again from 0 to 200 °C at 10 °C /min.

Thermal stability of lignin was studied by Thermogravimetric Analysis (TGA) on a Mettler Toledo 812e Thermogravimetric Balance under N_2 atmosphere and air as purge. About 2–4 mg of lignin were placed in aluminium crucibles and heated from 32 to 800 °C at 10 °C/min.

Esterification of Lignin

Most of the methods reported on lignin esterification are carried out by reaction with anhydrides in homogeneous solutions and with the addition of catalysts. The high reactivity of the anhydrides allows the modification of the aliphatic and phenolic hydroxyls present in the lignin [32].

The HW lignin was dissolved in acetic anhydride with an acetic anhydride/lignin weight ratio of 2:1. Then, 0.01 mL of N-methylimidazole per gram of lignin was added as catalyst. The reaction was carried out at 50 °C for 3 h in a round flask. Then, the reaction mixture was poured into cold deionized water and the esterified lignin was separated by centrifugation. The solid obtained was washed with deionized water and dried under vacuum in an oven at 50 °C. The product obtained is named HWE.

Pre-treatment of Lignin

(Unmodified and modified) lignin was previously subjected to a drying process in an oven with air circulation at a temperature of 60 °C for 24 h. Then, a reduction of the particle size was carried out in a ball mill and a granulometric classification was carried out to have lignin particles of size between 38 and 75 µm.

Lignin-Based Blends and Flexible Films

LLDPE/lignin blends given in Table 1 were prepared by melt extrusion using a HAAKE Rheomex P332 twin-screw extruder, 16 mm and L/D = 25 rate from Thermo Scientific located at Center of Chemical and Environmental Technology CQMA-IPEN/CNEN-SP. The temperature profile used during processing was 170/170/175/180/185/185 °C and the screw rotation was 60 rpm. The extrudates coming out of the extruder were cooled in water for a better dimensional stability of the pellets. Then, the pelletized LLDPE/lignin blends were fed into a HAAKE Rheomex blown

Table 1 Composition of blends

Name	Composition
LLDPE	100% LLDPE
SW-2.5	97.5% LLDPE–2.5% SW
SW-5	95% LLDPE–5% SW
SW-10	90% LLDPE–10% SW
HWE-2.5	97.5% LLDPE–2.5% HWE
HWE-5	95% LLDPE–5% HWE
HWE-10	90% LLDPE–10% HWE

film single-screw extruder, 16 mm and L/D = 25 rate from Thermo Scientific located at CQMA-IPEN/CNEN-SP and 0.045 mm in thickness films were obtained. The temperature profile used during the production of flexible films was 175/175/180/185/190/190 °C. Note that processability of LLDPE/HW lignin was not possible due to the low compatibility between the two components.

Characterization of LLDPE/Lignin Blends

The FTIR spectra of blends and neat LLDPE were acquired in a Shimadzu FTIR-8201 PC Fourier Transform Spectrophotometer in the 4000–400 cm^{-1} frequency region. KBr tablets containing 3%wt dry sample were prepared.

Thermal stability of blends was studied by TGA on a Mettler Toledo 812e Thermogravimetric Balance under N_2 atmosphere and air as purge. About 2–4 mg of sample were placed in aluminium crucibles and heated from 40 to 800 °C at 10 °C /min.

The morphological characterization of LLDPE/lignin blends was performed using a Phenon Pure Scanning Electron Microscope (SEM) at an accelerating voltage of 5 kV in low vacuum.

Biodegradability of LLDPE, SW-10 and HWE-10 was studied according to other authors [33]. The pellets coming out of the extruder were collected, crushed, and specimens of 40 × 20 mm were cut. The test was carried out in a flower pot containing farmland soil maintaining high relative humidity by daily sprinkling water at room temperature. Each specimen was buried in the soil for 30, 60 and 90 days, respectively; and then dug out and washed with water and dried. Weight loss was measured throughout the test.

Characterization of LLDPE/Lignin Films

The water absorption of films was measured according to other authors [34]. The samples were immersed in distilled water at room temperature. The test was carried out by periodically measuring sample weight gain as a function of immersion time for up to 35 days.

The opacity of the flexible films was measured by a GRETAG SPM 50 spectrophotometer (Gretag Data and Image Systems, Switzerland). The lightness value (L*) was obtained for films of constant thickness on a white background (white L*) and on a black background (black L*). The opacity was calculated according to Pires et al. [35].

Tensile properties were investigated using an INSTRON Model 4467 Universal Testing Machine according to ASTM D 882 standard. The grip distance was 50 mm and the clamp move speed for the test was 50 mm/min. All results were average values based on five specimens for each sample.

Results and Discussion

Characterization of (Unmodified and Modified) Lignin

Results of the moisture, ash, carbohydrates, purity and elemental composition of unmodified lignins are presented in Table 2.

The moisture of HW is 67% greater than SW. Impurities are higher for HW due to its higher ash and carbohydrate content. Carbohydrate content is negligible for SW and ash content is four times lower than HW.

As expected, carbon content of SW is 26% higher than for HW due to its lower ash content.

Nitrogen and sulfur content are similar for both lignins. The nitrogen content can be seen as an indicator for remaining proteins in the lignin. The sulfur content comes from the reagents used during the Kraft process.

The molar mass distributions (MMD) and average molecular weights obtained by SEC are given in Fig. 1 and Table 2, respectively. SW shows a higher weight average ($\overline{Mw}$), number average ($\overline{Mn}$), and dispersity ($\overline{Mw}/\overline{Mn}$) than HW [18].

SW and HW FTIR spectra are given in Fig. 2, O–H stretching band at 3400 cm^{-1} (peak 1), C–H stretching band at 2936 cm^{-1} (peak 2), aromatic skeleton stretching bands at 1600 cm^{-1}, 1510 cm^{-1} and 1430 cm^{-1} (peaks 4, 5 and 6,

Table 2 Characterization of lignin

	SW	HW
% Moisture	4.72	7.88
% Ash (dry basis)	4.31	17.84
% Carbohydrate (dry basis)	< 0.01	3.48
% Purity (dry basis)	96.7	78.7
C (%)	63.6	50.3
H (%)	5.92	4.13
N (%)	0.42	0.32
S (%)	2.13	1.93
$\overline{Mw}$(g mol^{-1})	8389	784
$\overline{Mn}$(g mol^{-1})	1800	716
Dispersity ($\overline{Mw}/\overline{Mn}$)	4.66	1.09
Aliphatic to phenolic OH ratio[a]	1.62	1.93
Phenolic OH[b] (OH/C9)	0.50	0.53
G/S[b]	84/16	60/40
Total (OH/C9)	1.31	1.55

All calculations have been done considering molecular weight of 180 g/mol and 210 g/mol for G and S moieties, respectively. C9 represents one phenyl propane unit

[a]From FTIR measurements

[b]From UV spectroscopic measurements

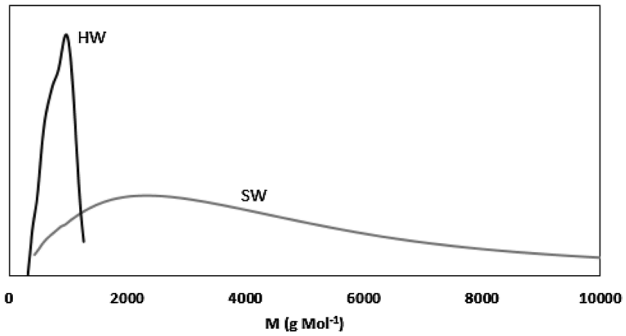

Fig. 1 SEC chromatograms of softwood (SW) and hardwood (HW) lignin

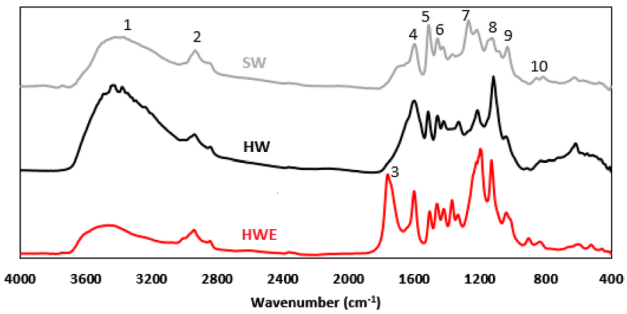

Fig. 2 FTIR spectra of unmodified (SW and HW) and chemically modified (HWE) lignin

respectively) and bands corresponding to G and S characteristic absorption at 1268 cm^{-1} (peak 7) and 1114 cm^{-1} (peak 8) are observed for SW and HW. The bands, C–H in-plane (1033 cm^{-1}, peak 9) and out-of-plane (810–855 cm^{-1}, peak 10) deformation vibration of C2, C5, and C6 in G moieties are also present. The intensity of S band in comparison to G characteristic signals is much higher for HW.

The aliphatic to phenolic OH ratio shown in Table 2 was calculated according to Eq. 2 [36].

$$\text{Aliphatic to phenolic OH ratio} = \frac{\text{A2936}}{\text{A1510}} \tag{2}$$

where A2936 and A1510 are the absorbances at 2936 cm^{-1} and 1510 cm^{-1}, respectively. The aromatic skeleton vibration at 1600 cm^{-1} was used for normalization.

The phenolic OH per average phenyl propane unit (C9) measured by UV spectroscopy are shown in Table 2. Phenolic OH are almost similar for SW and HW in accordance with the literature [19, 37]. As expected, SW is mainly composed by G moieties meanwhile HW has a lower G/S ratio [38]. The more condensed structure of SW, based almost exclusively on G units, explains its higher molecular weight.

Total OH given in Table 2 were calculated from the sum of aliphatic OH and phenolic OH. HW has 18.3% more OH than SW due to the greater amount of aliphatic OH that increases lignin polarity and hydrophilicity in agreement with the results of Sameni et al. [39].

All lignins are soluble in alkaline conditions. The solubility can be explained by the phenolic OH deprotonation [40]. Unlike SW, HW is soluble in water and insoluble in THF. The difference in water solubility can be explained by the lower average molecular weight and the greater polarity of HW in comparison with SW. The solubility of lignin in water increases with a decrease of molecular weight due to the higher disentanglement degree [41].

In order to improve the interfacial adhesion, HW was esterified to decrease lignin polarity and increase interactions with the matrix. FTIR spectrum of HWE is shown in Fig. 2. After chemical modification, ester groups were introduced into the lignin structure as it can be observed from the increased intensity of the characteristic signal corresponding to stretching vibration of carbonyl group (peak 3). Also, the band related to O–H at 3400 cm^{-1} becomes weaker and shifts to higher wavenumbers due to the decrease in interchain hydrogen bonding.

The acetylation reaction yield was calculated according to the procedure described by Gordobil et al. [42] using the Eq. 3.

$$\alpha = 1 - \left[\frac{\left(\frac{\text{A3400}}{\text{A2936}}\right)\text{HWE}}{\left(\frac{\text{A3400}}{\text{A2936}}\right)\text{HW}} \right] \times 100 \tag{3}$$

where A3400 and A2936 are the absorbances at 3400 cm^{-1} and at 2936 cm^{-1}, respectively. The performance achieved was 63.9% in accordance to Sameni et al. (2018) for a hardwood Kraft lignin [9].

DSC is the main method used to determine the glass transition temperature (Tg) of lignin. Lignin should have thermal properties similar to LLDPE to promote processing [43]. The Tg of lignin is more difficult to detect than in a synthetic polymer, due to the complex structure of the lignin macromolecule [44]. The Tg of lignin depends on various molecular factors such as interchain hydrogen bonding, rigid phenyl groups, crosslinking density, molecular weight and polydispersity [9]. After chemical modification, hydroxyl groups were replaced by ester substituents. This change affects the mobility of lignin molecules and the aggregation–dispersion behavior of the biopolymer particles in LLDPE matrix during the heat treatment procedure. In spite of the lower molecular weight and the higher impurities such as carbohydrate that could have a plasticizer effect, HW exhibited a Tg 20 °C higher than that of SW (162 °C and 142 °C, respectively). These results are in accordance with the higher aliphatic OH which makes HW mobility more difficult. HW cannot be redispersed during heat treatment

procedure due to its high Tg. The Tg of HWE is decreased substantially 29 °C lower than HW. The decrease in Tg can be ascribed to a reduction in the number of hydrogen bonds leading to a higher free volume that favors the mobility of the chains [42].

Figure 3 shows the TGA curves of the unmodified (SW and HW) and modified (HWE) lignin during the pyrolysis process. As observed by Brebu and Vasile [45], degradation occurs over a wide temperature range (150–800 °C) under nitrogen due to the complex lignin structure. At temperatures below 200 °C, the weight loss is associated to the volatilization of water present in lignin. As reported by Shi et al. (2012), low molecular weight products such as carbon dioxide, carbon monoxide and methane are also decomposed in this step [46]. In the second step, between 200 and 600 °C, the weight loss is due to a violent degradation of lignin.

The temperature for 50% of weight loss (T 50%) and the char (or unvolatized weight fraction) at 800 °C are shown at the top of Table 3.

The higher char residue for SW in comparison with HW is related to its more condensed structure. This difference between softwood and hardwood lignin was also reported by other authors [47, 48]. Although esterified lignin decomposes much faster than unmodified lignins the char residue is 15% more than HW. This difference is probably due to the lower average molecular weight of unmodified HW.

Characterization of LLDPE/Lignin Blends

FTIR

FTIR was used to study chemical structural changes between neat LLDPE and LLDPE/lignin blends. The spectra of LLDPE, SW-10 and HWE-10 are in Fig. 4. The FTIR spectrum of neat LLDPE show a characteristic C–H stretching band within the 3000–2840 cm^{-1} region (peak 1), medium strong C-H bending bands at 1465–1450 cm^{-1} (peak 3) and C–H out of plane bending within the 740–719 cm^{-1} region (peak 6) in accordance with Chandra et al. [49]. SW-10 spectrum show bands of the corresponding G and S characteristic absorption at 1268 cm^{-1} (peak 4) and 1114 cm^{-1} (peak 5). The absorption peak at wavenumbers of 1730 cm^{-1} (peak 2) for HWE-10 blend indicates the presence of C=O from the esterified lignin.

TGA

Figure 5 shows TGA curves for LLDPE/SW blends. Similar curves were obtained for LLDPE/HWE blends. Parameters such as T50% and char are presented in Table 3. For the neat LLDPE, thermal decomposition takes place in a single step between 350 and 480 °C. This behavior is due to the cleavage of carbon atoms (C–C) in the main chain of the polymer as reported by Shebani et al. [50]. At the end of the test, the residue is 0.10%. The addition of lignin causes a shift towards higher temperatures respect to neat LLDPE in accordance with the fire-retardant property of lignin. The increased thermal stability of blends can be attributed to the complex phenyl propane structure of lignin.

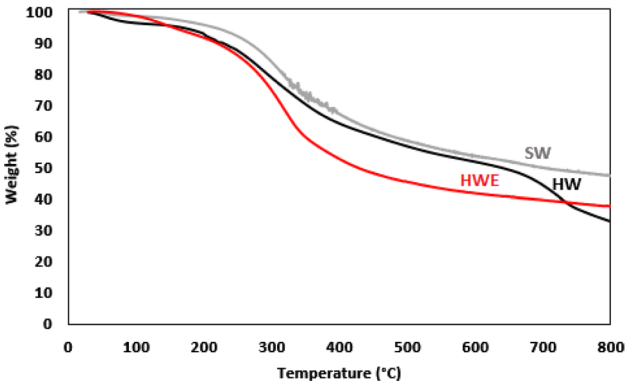

Fig. 3 TGA curves of unmodified (SW and HW) and chemically modified (HWE) lignin

Table 3 Thermal properties of unmodified (SW and HW), chemically modified (HWE) lignin, neat LLDPE and lignin-based blends

	T 50% (°C)	Char (%)
Lignins		
SW	678	47
HW	639	33
HWE	427	38
Blends		
LLDPE	415	0.10
SW-2.5	452	0.76
SW-5	445	0.77
SW-10	446	0.89
HWE-2.5	453	0.11
HWE-5	442	0.18
HWE-10	444	0.45

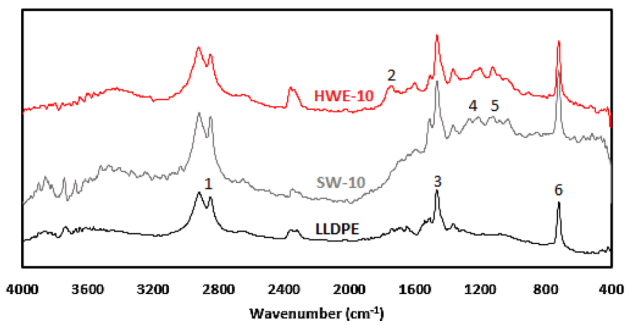

Fig. 4 FTIR spectra: LLDPE and blends with 10% of lignin

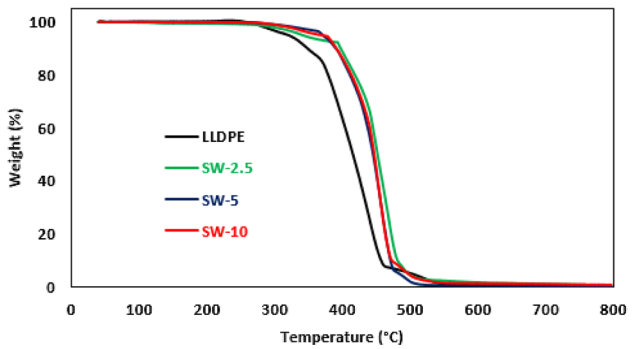

Fig. 5 TGA curves: LLDPE and LLDPE/SW blends

LLDPE/SW blends show higher char than LLDPE/HWE due to the more condensed structure of SW in concordance with thermal stability of lignin. Also, the char increases with lignin increase. This behavior has also been observed in other lignin-based materials [42].

SEM

SEM micrographs of the fractured surface for LLDPE/SW blend with 10% of lignin are shown in Fig. 6. Figure 7 shows the surface morphology of LLPDE/HWE blend with 10% of lignin. The incorporation of unmodified SW lignin in LLDPE shows a rough texture on the blends (Fig. 6) compared to HWE which exhibits a smoother surface (Fig. 7) due to the better compatibility between the two compounds. Lignin aggregation–dispersion behavior mainly depends on its initial particle size and the ability of aggregation under dry state [51]. Lignin self-aggregates of approximately 20–30 µm are observed in LLDPE/SW and LLDPE/HWE suggesting a reduction of its original size (30–75 µm) after processing. However, HWE lignin seems to be slightly better dispersed than SW. After chemical modification, functional ester groups were introduced in HW lignin affecting the chain motion of lignin macromolecule, lowering its Tg, and changing the aggregation–dispersion behavior of lignin in LLDPE matrix when heat is applied during processing.

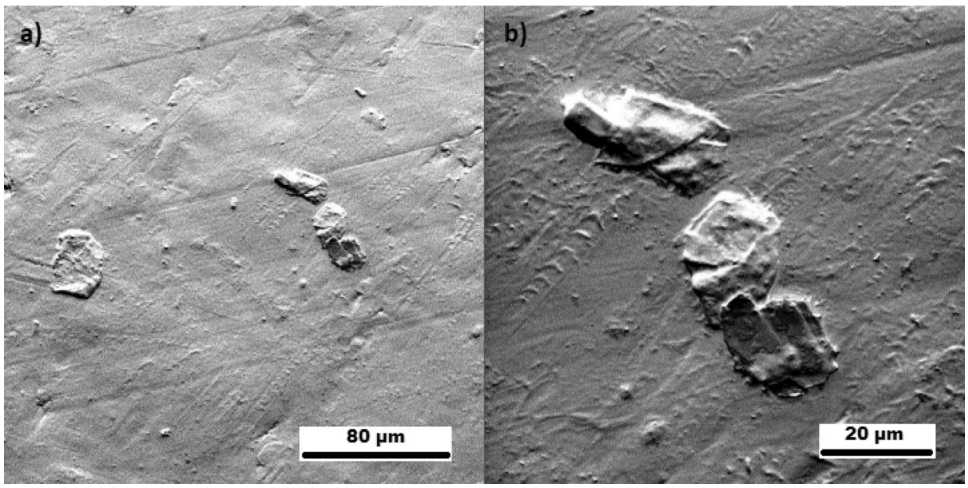

Fig. 6 SEM images of SW-10 blend. **a** 1000 ×, and **b** 3000 ×

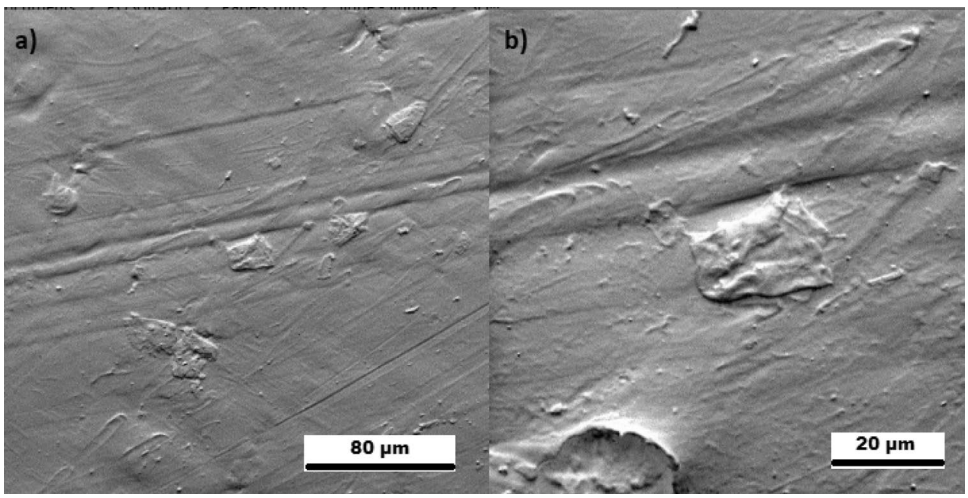

Fig. 7 SEM images of HWE-10 blend. **a**1000 ×, and **b** 3000 ×

This suggests an improved dispersion of HWE in LLDPE matrix. In contrast, hydrogen bonds between HWE molecules and the difference in polarity between HWE and non-polar LLDPE matrix promote lignin self-aggregation. It is known that hydrogen bonds formed by aliphatic hydroxyl groups are stronger than those formed by hydroxyl phenolic groups [52]. Also, the non-covalent π-π interactions between phenyl rings in lignin contribute to its aggregation. The compatibility of LLDPE/lignin blends depends on the competition between lignin self-aggregation and lignin-LLDPE interaction. Assemblies of aggregates form agglomerates in LLDPE/SW blends. The lower lignin dispersion is attributed to the high molecular weight of SW that decrease lignin motion. In addition, the more intensive agglomeration suggests high intermolecular interactions between aggregates.

Biodegradability Test

Figure 8 shows weight loss measurements after soil burial test. Weight loss was almost three times higher for HWE-10 and twice for SW-10 in comparison with neat LLDPE after 90 days of soil burial. Low molecular weight and the presence of ester groups in lignin increase biodegradability of lignin-based materials.

Characterization of LLDPE/Lignin Films

Water Absorption

Water absorption is an important characteristic both during the useful life and at the end life of a material. Materials are intended to be hydrophobic for mulch films applications and to absorb water at the end of its useful period in order to promote biodegradation [53]. For films containing 2.5%, 5% and 10% of SW, the percentages of final water absorption are 2.30%, 2.61% and 2.77% respectively. This can be attributed to the OH groups in lignin that makes it more hydrophilic than neat LLDPE. Furthermore, as reported, it could be assumed that the amorphous structure of lignin loosens the network structure of the blend [54]. Water absorption increases with the increase of HWE in higher proportions. Neat LLDPE and blends containing 2.5%, 5% and 10% esterified lignin absorbed 1.18%, 1.71%, 2.13% and 3.71% of water, respectively. For lignin content below 5%, water absorption is higher for LLDPE/SW in comparison with LLDPE/HWE, but above 5% water absorption is lower. These results suggest a greater effect of lignin polarity over molecular weight for blends with low proportions of lignin and vice versa. During the first 23 days, water absorption for HWE-2.5 is almost similar to the corresponding neat LLDPE, ensuring hydrophobicity for its application and promoting its degradability at the end of its useful life.

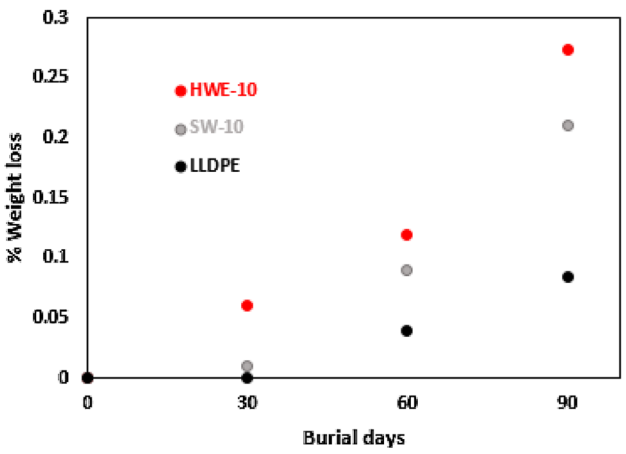

Fig. 8 Soil burial test

Opacity

Extrusion processes force molten polymer through a printer nozzle at high wall shear rates (> 100 s^{-1}) that lead to flow-induced crystallization. Thus, the generation of small crystals that confer transparency and stiffness is promoted. The values of black L*, white L* and opacity of films are given in Table 4. The opacity of LLPDE/SW films is slightly greater than LLDPE/HWE probably to the lower dispersion of SW as observed in SEM. As larger quantities of lignin are added opacity of the films increases. Opacity promotes absorption of incident solar radiation and weed control will be more effective.

Tensile Tests

The tensile stress–strain curves for LLDPE and LLDPE/SW films are shown in Fig. 9. Four typical regions can be observed on the curves. First, stress is almost linear and the slope is a measure of the elastic modulus of the material. The second region corresponds to the "yield point", associated with the beginning of yielding in the specimen. After

Table 4 Opacity of LLDPE/SW, LLDPE/HW and LLDPE films

	Black L*	White L*	% Opacity = $\frac{\text{Black } L^*}{\text{white } L^*} \times 100$
LLDPE	44.04	97.92	44.97
SW-2.5	42.55	91.26	46.62
SW-5	42.33	90.54	46.75
SW-10	40.40	84.90	47.58
HWE-2.5	43.46	94.74	45.10
HWE-5	42.73	93.27	45.81
HWE-10	41.23	88.03	46.83

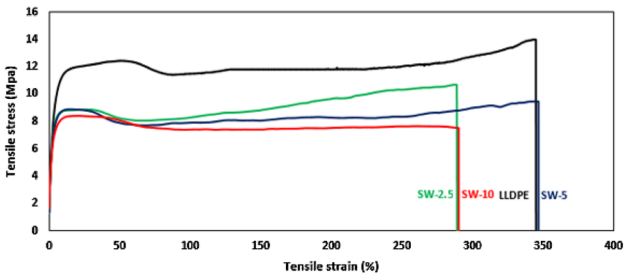

Fig. 9 Tensile stress–strain curves for LLDPE/SW and LLDPE films

yielding, crystalline reorientation takes place and there is an additional extension with approximately constant stress (third region). In the fourth region, the polymer chains approach full alignment and stress increases until break. The mechanical properties of neat LLDPE, LLDPE/SW and LLDPE/HWE films are shown in Table 5. In order to obtain comparisons between materials, the response variables (tensile strength at break, elongation at break, Young´s modulus) were subjected to analysis of variance (ANOVA) and the results were compared by Fisher's test at a significance level of 0.05. INFOSTAT statistical software (2017 version) was employed for the statistical treatment. Means are significantly different if $p < 0.05$. The results are presented in the Table 6. No significant differences in elongation at break were found between neat LLPDE and LLPDE/lignin films with 2.5% HWE and up to 5% SW but tensile strength decreased approximately 30%. Self-aggregates and agglomerates cannot share the external stress leading in a poor distribution of stress due to the lack of interfacial adhesion which causes the deterioration of the performance. Young's modulus is greater for LLPDE/SW than LLPDE/HWE. This result is in accordance with many authors who have demonstrated that the addition of unmodified lignin imparts stiffness to the polymeric matrix but a reduction in tensile strength and elongation at break [55, 56]. The reduction in stiffness for LLPDE/HWE is in accordance with Dehne et al. (2016) for esterified Kraft hardwood lignin/HDPE [18] and with Luo et al. (2017) for esterified Kraft softwood lignin/PP [27]. The low Tg (low polarity and molecular weight) of HWE promotes lignin mobility due to a missing interaction between lignin and polyolefin according to Toriz et al. [57] and entails a redispersion or improved compatibility under stress.

Conclusions

Lignin-based polyethylene mulch films with improved opacity, thermal and biodegradability properties, and good mechanical and water absorption performance were obtained as a sustainable economic and environmental alternative to LLDPE films. Properties of the films depend on lignin structure and its interaction with LLDPE. Lignin Tg increases with an increase in aliphatic OH. A difference of 41 °C between the Tg of HW and the melting temperature of LLPDE entailed non-processable LLPDE/HW blends. Functionalization by esterification was performed in order to increase the lignin-matrix compatibility. Processable films exhibited lignin self-aggregates. Stiffness was greater for LLPDE/SW than for LLPDE/HWE meanwhile tensile strength and elongation at break decreased with lignin increase. Elongation at break of LLPDE blends with 2.5% HWE and up to 5% SW were statistically comparable to neat LLDPE in spite of a decrease in tensile strength. Also, HWE-2.5 exhibited statistically comparable water absorption with neat LLDPE during the first 23 days.

Table 5 Tensile test of LLDPE/SW, LLDPE/HW and LLDPE films

Sample	Tensile strength at break (MPa)	Elongation at break (%)	Young's modulus (MPa)
LLDPE	14.06 ± 1.4	357.41 ± 15.3	323.45 ± 43.1
SW-2.5	9.75 ± 2.4	339.22 ± 43.1	369.52 ± 23.7
SW-5	9.45 ± 2.1	348.35 ± 23.7	352.66 ± 42.4
SW-10	7.51 ± 2.6	290.25 ± 28.5	342.70 ± 50.4
HWE-2.5	9.42 ± 2.0	351.33 ± 21.5	221.27 ± 22.8
HWE-5	8.69 ± 1.7	212.00 ± 16.0	226.34 ± 50.1
HWE-10	7.31 ± 1.8	242.98 ± 19.9	192.86 ± 38.5

Table 6 Statistical comparison of the results obtained in tensile tests

Tensile strength at break (MPa)	LLDPE > HWE-2.5 = SW-2.5 = SW- 5 > HWE-5 > HWE-10 = SW-10
Elongation at break (%)	LLDPE = HWE-2.5 = SW-2.5 = SW-5 > SW-10 > HWE-10 > HWE-5
Young's modulus (MPa)	SW-2.5 > SW-5 = SW-10 > LLDPE > HWE-2.5 = HWE-5 > HWE-10

Acknowledgements This research was financially supported by Universidad Tecnológica Nacional (Grant No. PID IPAISF0004433TC and PID IPTUNRE0004309) and CONICET (Grant. No P-UE 2016) from Argentina, and São Paulo Research Foundation—FAPESP. The authors would like to thank to Marcelo Brandolini (INTEC) and Matias Molinaro and Evelin Giampaoli (WINDSA) for the help and support during this research.

References

1. Kasirajan S, Ngouajio M (2012) Agron Sustain Dev 32:501
2. Dorigato A, Pegoretti A, Fambri L, Lonardi C, Kola J (2011) eXPRESS Polym Lett 5:23
3. Niaounakis M, Kontou E (2005) J Polym Sci B 43:1712
4. Guichon O, Seguela R, David L, Vigier C (2003) J Polym Sci B 41:327
5. Miao C, Hamad WY (2017) J Appl Polym Sci 34:1–10
6. Pucciariello R, Villani V, Bonini C, D'Auria M, Vetere T (2004) Polymer 45:4159
7. Collins M, Nechifor M, Tanasa F, Zanoaga M, McLouglhin A, Strozyk M, Culebras M, Teaca C (2019) Int J Biol Macromol 131:828
8. Kun D, Pukansky B (2017) Eur Polym J 93:618
9. Sameni J, Jaffer SA, Sain MT (2018) Compos A 115:104
10. Borysiak S, Klapiszewski Ł, Bula K, Jesionowski T (2016) J Therm Anal Calorim 126:251
11. Bula K, Klapiszewski Ł, Jesionowski T (2019) Polym Test 77:105911
12. Bula K, Klapiszewski Ł, Jesionowski T (2015) Polym Compos 36:913
13. Bula K, Kubicki G, Jesionowski T, Klapiszewski Ł (2020) Materials 13:1
14. Bula K, Kubicki G, Kubiak A, Jesionowski T, Klapiszewski Ł (2020) Polymers 12:1156
15. Grząbka-Zasadzińska A, Klapiszewski Ł, Bula K, Jesionowski T, Borysiak S (2016) J Therm Anal Calorim 126:263
16. Klapiszewski Ł, Bula K, Dobrowolska A, Czaczyk K, Jesionowski T (2019) Polym Test 73:51
17. Klapiszewski Ł, Bula K, Sobczak M, Jesionowski T (2016) Int J Polym Sci 1:1
18. Dehne L, Vila Babarro C, Saake B, Schwarz KU (2016) Ind Crops Prod 86:320
19. Tejado A, Peña C, Labidi J, Echeverria JM, Mondragon I (2007) Bioresour Technol 98:1655
20. Laurichesse S, Avérous L (2014) Prog Polym Sci 39:1266
21. El Mansouri NE, Salvadó J (2006) Ind Crops Prod 24:8
22. Samal SK, Fernandes EG, Corti A, Chiellini E (2009) Int J Mater Prod Technol 36:62
23. Ghozali M, Triwulandari E, Haryono A, Yuanita E (2017) IOP Conf Ser 223:012008
24. Gordobil O, Robles E, Egüés I, Labidi J (2016) RSC Adv 6:86909
25. Vila C, Santos V, Saake B, Parajó JC (2016) BioResources 11:5322
26. Maldhure AV, Chaudhari AR, Ekhe JD (2010) J Therm Anal Calorim 103:625
27. Luo S, Cao J, McDonald AG (2017) Ind Crops Prod 97:281
28. Barana D, Orlandi M, Zoia L, Castellani L, Hanel T, Bolck C, Gosselink R (2018) ACS Sustain Chem Eng 6:11843
29. Virtanen S, Chowreddy RR, Irmak S, Honkapää K, Isom L (2017) J Polym Environ 25:1110
30. Gartner A, Gellerstedt G (1999) Nord Pulp Pap Res J 14:163
31. Faix BO, Argyropoulos DS, Robert D, Neirinck V (1994) Holzforschung 48:387
32. Yang Liu L, Hua Q, Renneckar S (2019) Green Chem 21:3682
33. Kumar R, Yakubu MK, Anandjiwala RD (2010) eXPRESS Polym Lett 4:423
34. Pichaiyut S, Nakason C, Wisunthorn SB (2018) J Polym Environ 26:2855
35. Pires C, Ramos C, Teixeira B, Batista I, Nunes ML, Marques A (2013) Food Hydrocoll 30:224
36. Malutan T, Nicu R, Popa V (2008) BioResources 3:13
37. Brodin I, Sjoholm E, Gellerstedt G (2009) Holzforschung 63:290
38. Fitigau IF, Peter F, Boeriu CG (2013) Int J Chem Mol Nucl Mater Metall Eng 7:98
39. Sameni J, Krigstin S, Sain M (2017) BioResources 12:1548
40. Schutyser W, Renders T, Van den Bosch S, Koelewijn S, Beckham GT, Sels BF (2018) Chem Soc Rev 47:852
41. Melro E, Alves L, Antunes F, Medronho B (2018) J Mol Liq 265:578
42. Gordobil O, Egüés I, Llano-Ponte R, Labidi J (2014) Polym Degrad Stab 108:330
43. Schorr D, Diouf PN, Stevanovic T (2014) Ind Crops Prod 52:65
44. Lisperguer J, Perez P, Urizar S (2009) J Chil Chem Soc 4:460
45. Brebu M, Vasile C (2010) Cell Chem Technol 44:353
46. Shi Z, Xiao L, Xu F, Sun R (2012) J Appl Polym Sci 125:3290
47. Dávila I, Gullón B, Labidi J, Gullón P (2019) Renew Energy 142:612
48. Lourençon T, Hansel F, Da Silva T, Ramos L, Munis G, Magalhaes W (2015) Sep Purif Technol 154:82
49. Chandra R, Rustgi R (1997) Polym Degrad Stab 56:185
50. Shebani AN, Van Reenen AJ, Meincken M (2009) J Compos Mater 43:1305
51. Jiang C, He H, Yao X, Yu P, Zhou L, Jia D (2018) J Appl Polym Sci 135:45759
52. Zhao W, Xiao LP, Song G, Sun RC, He L, Singh S, Simmons BA, Cheng G (2017) Green Chem 19:3272
53. Nguyen DM, Do TVV, Grillet AC, Thuc HH, Thuc CNH (2016) Int Biodeterior Biodegrad 115:257
54. Luo S, Cao J, McDonald AG (2018) Ind Crops Prod 121:169
55. Anwer MAS, Naguib HE, Celzard A, Fierro V (2015) Compos B 82:92
56. Ghozali M, Sinaga PDB, Maranata S, Rohmah ENS (2016) World Chem Eng J 1:11
57. Toriz G, Denes F, Young RA (2002) Polym Compos 23:806